INT. J. REMOTE SENSING, 2005, preview article

Using satellite imagery and GIS for land-use and land-cover change mapping in an estuarine watershed

XIAOJUN YANG* and ZHI LIU
Department of Geography, Florida State University, Tallahassee, FL 32306, USA

The degradation of world-wide estuarine ecosystems as a result of accelerated human population growth accompanied by agricultural, industrial and urban development justifies a strong need to find efficient ways to manage and protect these sensitive environments. Starting from 2001, the authors have been involved in an interdisciplinary research project aiming to develop environmental indicators for integrated estuarine ecosystem assessment in the Gulf of Mexico. As part of this project, a study was conducted to characterize land-use and land-cover changes with the Pensacola estuarine drainage area as a case. The Pensacola bay was targeted because it is one of few exemplary large river-driven estuarine systems across the northern Gulf of Mexico. The study had two major sections. The first part was dedicated to the development of an improved method for coastal land-use and land-cover mapping, which was built upon hierarchical classification and spatial reclassification. An image scene was separated into urban and rural regions early in the classification, with a 'mask' defined by road intersection density slices combined with road buffers. Each part was classified independently in its most effective context and, later, both were merged to form a complete map. In spatial reclassification, image interpretation procedures, auxiliary vector data and a variety of Geographical Information System (GIS) functions were synthesized to resolve spectral confusion and improve mapping accuracy. This method was used to map land use and land cover from Landsat Thematic Mapper/Enhanced Thematic Mapper Plus (TM/ETM+) imagery for 1989, 1996 and 2002, respectively. The accuracy assessment shows that the overall classification errors were less than 10%. The second part focused on the analysis of the spatio-temporal dynamics of estuarine land-use and land-cover changes by using post-classification comparison and GIS overlay techniques. The project has revealed that a substantial growth of low-density urban land occurred in the lower drainage basin in connection with population and housing growth, as well as a significant increase of mixed forest land in the upper watershed as a result of active logging and harvesting operations. These growths were achieved at the cost of evergreen forest and wetlands, thus compromising safeguards for water quality, biodiversity of aquatic systems, habitat structure and watershed health in the Pensacola estuarine drainage area.

1. Introduction and research objectives

Estuaries, the transitional zones where salt water from the sea mixes with fresh water flowing from the inland streams, belong to the most dynamic ecosystems on Earth. At the same time, estuaries are the foci of human settlement, industry and tourism. Coastal human population growth accompanied by agricultural, industrial and

*Corresponding author. Email: xyang@fsu.edu

International Journal of Remote Sensing
ISSN 0143-1161 print/ISSN 1366-5901 online © 2005 Taylor & Francis
http://www.tandf.co.uk/journals
DOI: 10.1080/01431160500219224

urban development has led to an unparalleled acceleration of contaminant and nutrient inputs into coastal estuaries and their watersheds, thus exacerbating environmental stress and degradation of estuarine ecosystems throughout the world (Lakshmi and Rajagopolan 2000, Bowen and Valiela 2001, Shi *et al*. 2002, Dojiria *et al*. 2003, Finkl and Charlier 2003, Shi and Singh 2003). Therefore, there is a strong need to find efficient ways to manage and protect these highly sensitive ecosystems (Niemi *et al*. 2004).

Environmental problems in estuarine ecosystems can sometimes be ascribed to excess nutrients flowing from upstream watersheds (NRC 2000). Understanding the cause of nutrient over-enrichment (i.e. eutrophication) needs an integrative effort within the context of watershed dynamics (Boesch 2001). Landscape characterization affects coastal water quality by altering sediment, chemical loads and watershed hydrology (Basnyat *et al*. 1999). Therefore, information on land-use and land-cover change is indispensable for integrated estuarine watershed assessment.

Thematic assessments of estuarine land-use and land-cover changes involve procedures of monitoring and mapping which require effective methods and techniques. Conventional survey and mapping methods cannot deliver necessary information in a timely mode. Remote sensing, given its cost effectiveness and technological robustness, has been increasingly used for characterizing coastal areas and analysing their land-use and land-cover changes (Rao *et al*. 1999, Gonzalez 2001, Chen 2002, Shi *et al*. 2002, O'Hara *et al*. 2003, Ruiz-Luna and Berlanga-Robles 2003). On the other hand, estuarine environments are characterized by erratic climate conditions and complex landscape structure. The high humidity in coastal areas makes it difficult to obtain cloud-free images. The presence of complex urban impervious materials and agricultural lands, along with a variety of wetlands and vegetation covers, causes substantial inter-pixel and intra-pixel changes in estuarine environments. These factors are collectively challenging the applicability and robustness of remote sensing technologies for coastal landscape change mapping.

Over the past decades, there have been significant improvements in the availability of remotely sensed data and in their spectral and spatial resolution, along with substantial research efforts directed to improve the performance of automated mapping in heterogeneous landscapes (O'Hara *et al*. 2003, Barnsley and Barr 1996, Yang 2002, Herold *et al*. 2003, Schmidt *et al*. 2004). Nevertheless, these technologies and methods can vary greatly with the change in image characteristics and the circumstance for targeted studies (Campbell 2002). For a specific application, an analyst must identify an appropriate method in order to produce satisfactory results with acceptable accuracy. Therefore, further efforts will be needed in order to consolidate the applicability of remote sensing for land-use and land-cover change mapping in highly dynamic estuarine environments.

This study investigates the usefulness of satellite remote sensing and Geographical Information System (GIS) technologies for coastal land-use and land-cover change characterization with the Pensacola estuarine drainage area (PEDA) as a case. The study area has historically supported a rich and diverse ecosystem, productive fisheries and considerable recreational opportunities in northwestern Florida (EPA 1999). During the past decade, this area has witnessed significant population and economic growth, which has led to exacerbations of point and non-point source pollution, hydrological alterations and direct habitat destruction throughout the watershed. These have provoked concerns over degradation of the health of the

ecosystem in the study area. Starting from 2001, the authors have been involved in an interdisciplinary research project CEER-GOM (**C**onsortium for **E**stuarine **E**coindicator **R**esearch for the **G**ulf **O**f **M**exico). Project CEER-GOM is funded by the US Environmental Protection Agency (EPA) through the Estuarine and Great Lakes (EaGle) programme, which has the objective to develop environmental indicators for estuarine ecosystem integrative assessment in the Gulf of Mexico. Pensacola Bay, as one of the three exemplary large-scale river-driven estuarine systems across the northern Gulf of Mexico, has been selected for detailed research by Project CEER-GOM. This article examines the land-use and land-cover change in PEDA by using satellite remote sensing and GIS technologies. The specific objectives were: (i) to identify a method for coastal land-use and land-cover mapping; (ii) to apply this method to create a time series of land-use and land-cover maps; and (iii) to analyse the spatio-temporal dynamics of coastal land-use and land-cover changes.

2. Research methodology

The research methodology can be divided into the following major components: (i) data acquisition and collection; (ii) data preprocessing; (iii) classification scheme design; (iv) hierarchical classification; (v) spatial reclassification; (vi) accuracy assessment; and (vii) land-use and land-cover change analysis. Collectively, the first six parts were to map coastal land use and land cover through hierarchical classification and spatial reclassification. The last part was for change detection. This section provides the technical details for the first six procedures, along with a brief description of the study area.

2.1 *Study area*

The geographical coverage of PEDA includes the majority of Escambia, Santa Rosa and Okaloosa counties, the northwestern Walton County in Florida, as well as portions of Escambia, Covington, Monroe and Conecuh counties in Alabama (figure 1). The study area is actually the estuarine portion of Pensacola Bay drainage basin, which is approximately 50% of the total watershed area (NFWMD 1997). The entire basin discharges into the Gulf of Mexico through a narrow pass at the mouth of Pensacola Bay. The PEDA is defined according to National Oceanic & Atmospheric Administration (NOAA)'s Coastal Assessment Framework (CAF). CAF is a GIS-based digital spatial framework designed for managers and analysts to organize information on the nation's coastal, near-ocean and Great Lakes' resources (NOAA 1999). The PEDA has a total area of 9119 km^2. This represents 8643 km^2 of upstream watershed and 476 km^2 of bays, fitting well within a whole scene ($185 \times 185\ km^2$) of the Landsat Thematic Mapper/Enhanced Thematic Mapper Plus (TM/ETM+) imagery.

Physiographically, the PEDA lies within the Coastal Plain province, which is underlain mainly by beds of sand, silt and clay that dip gently seaward (Marsh 1966). The estuarine embayments are within the Gulf Coastal Lowlands subdivision and contain a series of parallel terraces rising from the coast in successively higher levels. Much of the area is less than 30 m above sea level. PEDA includes three major river systems – Escambia, Blackwater and Yellow rivers. The climate is humid subtropical with generally warm temperatures.

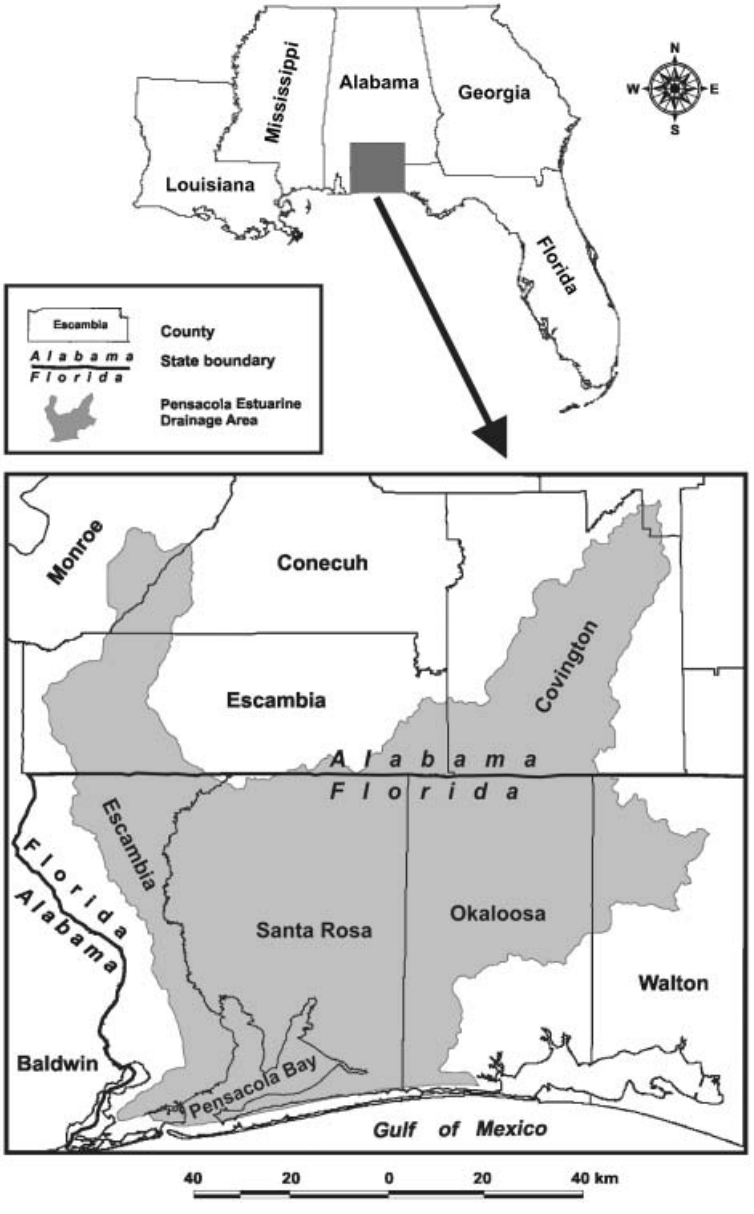

Figure 1. Location of the study area.

2.2 *Data acquisition and collection*

The primary data used in this study were remotely sensed images. There are a variety of imagery types that could be used and, normally, images with higher spatial and/or spectral resolutions are preferred for coastal land-use and land-cover mapping. But higher resolution data are generally more expensive. Therefore, there is a cost-effectiveness issue that needs to be considered for any remote sensing project. Because of the budget constraint and the time availability, Landsat TM and ETM+

imagery were chosen as the primary data. Although rather difficult, it was possible to acquire a predominantly cloud-free scene of Landsat data covering the Pensacola metropolitan area from USGS EROS Data Center for 1989, 1996 and 2002, respectively. The specific dates, types of images, Landsat satellite series number, nominal spatial resolution, number of bands and other environmental parameters are summarized in table 1.

To facilitate satellite-based coastal landscape change mapping, a range of reference data were collected:

(i) USGS 1 m DOQQs (Digital Ortho Quarter Quads) in black-and-white and colour formats (USGS 1996);
(ii) USGS 1 : 24 000 digital topographical maps (USGS 2004a);
(iii) ESRI 2002 road networks (ESRI 2003);
(iv) National Wetland Inventory (NWI) 1 : 250 000 wetlands dataset for 1992 (USFWS 2004);
(v) political boundaries (such as counties and state boundaries) from ESRI 2002 Data and Maps (ESRI 2003);
(vi) USGS 1: 250 000 hydrological unit boundaries (USGS 2004b);
(vii) Florida Department of Environmental Protection (FDEP) 1995 digital land-use map created through airphoto interpretation for counties within Florida (FDEP 2004); and
(viii) USGS digital land-use and land-cover map derived from automated image classification for 2001 (USGS 2004c).

In addition, extensive field surveys were conducted through five major routes (figure 2), which were guided with a differential Global Positioning System (GPS) receiver. More than 600 digital photos were taken for different types of land use and land cover, along with thousands of GPS point readings. The data collected during the field surveys were used for three major purposes: (i) to determine the major types of land use and land cover in the study area, which helped design a land-use and land-cover classification scheme; (ii) to associate the ground 'truth' of a specific type of land use and land cover with its imaging characteristics, which helped classify images and produce land-use and land-cover maps; and (iii) to collect sufficient

Table 1. Summary of the characteristics of the satellite images used.

Date	Type of image	Landsat No.	Spatial resolution (m)	No. of bands*	Sun elevation (°)	Sun azimuth (°)	rms. error (GCP No.)	Radiometric normalization
6 April 1989	TM	5	30	6	52.73	124.03	0.089 (16)	Yes
9 April 1996	TM	5	30	6	50.05	117.51	0.078 (16)	Reference
20 May 2002	ETM+	7	15†, 30	7	66.00	109.30	Reference	Yes

*Thermal bands were not used in actual classification
†The panchromatic band has a resolution of 15 m.

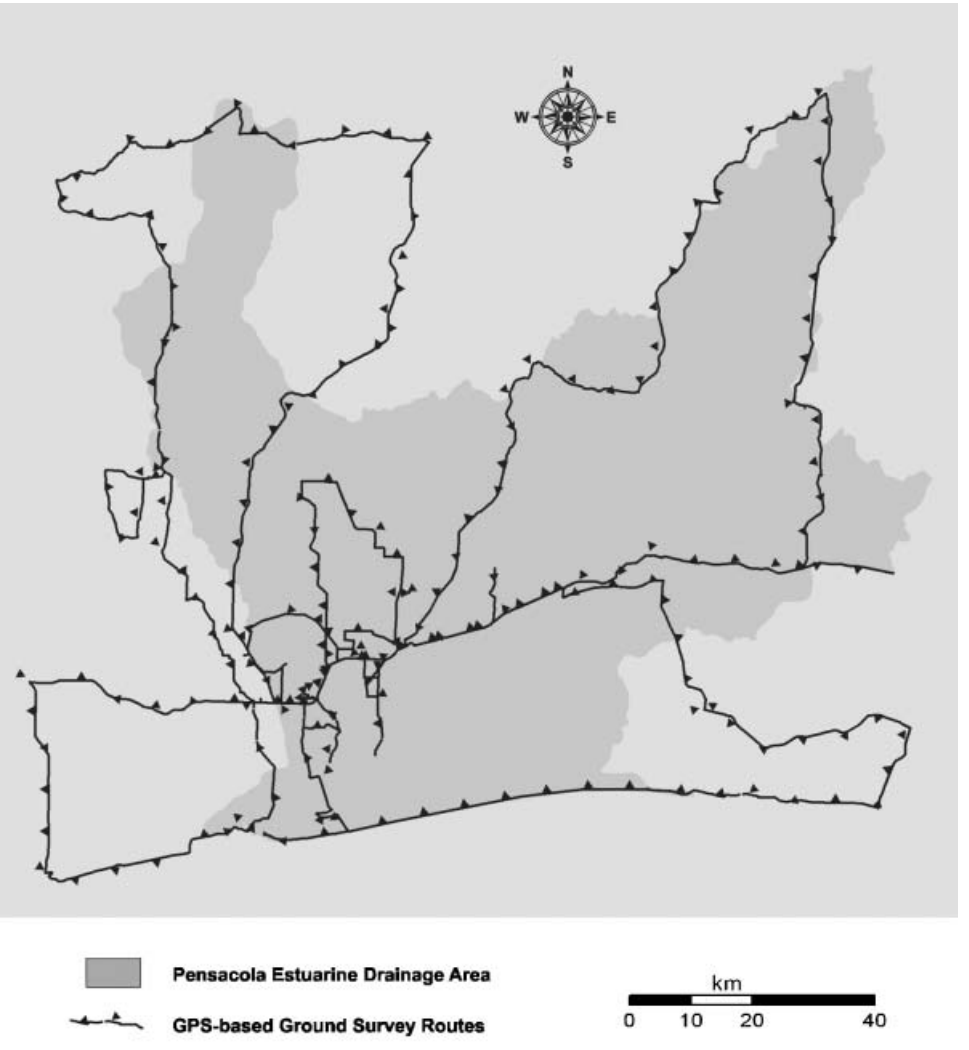

Figure 2. GPS-based field survey routes. The boundary of the Pensacola estuarine drainage area is shown. The total length of these routes is more than 1500 km.

ground data for use in accuracy assessment of the land-use and land-cover maps. Therefore, fieldwork has been an essential component for data acquisition and collection.

2.3 *Image preprocessing*

Both geometric rectification and radiometric normalization were conducted in the phase of image preprocessing. The georeferencing strategy adopted here was actually an image-to-image registration. First, the 2002 ETM+ image was rectified by using USGS 1: 24000 digital topographic maps. The ETM+ image was georeferenced to the UTM (Universal Transverse Mercator) map projection (Zone 16), NAD83 horizontal datum and GRS84 ellipsoid. Then, this image was used as the reference to rectify the images for 1989 and 1996, respectively. For both cases, 16

good ground control points were used and the rms. errors were less than 0.5 pixel (table 1).

Radiometric normalization is used to suppress the spectral differences that are caused because of factors such as atmospheric absorption and scattering, sensor-target-illustration geometry, sensor calibration and image data processing procedures, which tend to change over time. This is a critical procedure for any change analysis (Jensen 2004). There are a variety of radiometric normalization methods and their performance can alter according to the variations in the pattern of land-use and land-cover distribution, water–land distribution, topographic relief, similarity between the reference and subject scenes, and sample size (Yang and Lo 2000). After a careful examination on the Pensacola image scenes, the radiometric normalization method developed by Hall *et al.* (1991) was adopted because this method is particularly suitable for scenes characterized by relatively even terrain with some deep-water bodies and highly reflective urban built-up land (Yang and Lo 2000). The Hall method of radiometric normalization using radiometric control sets was applied to the 1989 and 2002 scenes with the 1996 scene as the reference.

2.4 *Classification scheme design*

Based on the research objectives, image spatial resolution and field surveys, a modified version of the Anderson scheme (Anderson *et al.* 1976) was developed.

- *Low density urban (LDU)* consists of approximately 40–70% (impervious) construction materials, which are typically residential development including single/multiple family houses and public rental housing estate, as well as local roads and small open (transitional) space as can be always found in a residential area; it also contains a various amount of vegetation cover.
- *High density urban (HDU)* is characterized by approximately 70–100% (impervious) construction materials, which are typically commercial and industrial buildings with large open roofs as well as large open transportation facilities (e.g. large airports, parking lots, and multi-lane interstate/state highways); it also includes military bases, tourism and recreational facilities, and a small percentage of residential development residing in the city cores.
- *Agricultural land (AGL)* is characterized by crops, pastures and other herbaceous vegetation, including lands that are regularly mowed for hay or grazed by livestock and regularly tilled and planted cropland; it may contain small parks and golf courses.
- *Evergreen forest (EGF)* includes coniferous forests (vegetative species such as pine and cedar).
- *Mixed forest (MXF)* consists of evergreen and deciduous species mixed with a various amount of shrubs, brushes and young trees.
- *Woody wetlands (WWL)* include hardwood, mixed forest and shrubs, which are distributed along rivers and bays.
- *Emergent herbaceous wetlands (EHW)* is characterized by tall grasses such as black needle rush; it is also called swamp, salt marsh and brackish marsh.
- *Barren land (BCH)* consists of the areas of sparse vegetation cover (less than 20%), including beaches, clearcuts and transactional lands that are likely to change or be converted to other uses in the near future.
- *Water (WTR)* consists of all areas of open water, generally with greater than 95% cover of water, including streams, rivers, lakes, reservoirs and bays.

2.5 *Hierarchical classification*

After a careful examination of the image scenes acquired, it was found that some types of land use and land cover tend to be spectrally similar. For example, urban built-up land shows similar spectral reflectance to barren land and several types of agricultural land. This is actually a form of the spectral confusion problem that was described by Yang (2002). If a pixel-by-pixel classification algorithm is used with all available image signals considered, the pixels with similar spectral reflectance would be grouped together, regardless of their associated uses. This would augment the level of classification errors. Clearly, spectral confusion is the major barrier to achieving adequate accuracy using a per-pixel-based classification method from remotely sensed images with middle-size spatial resolutions and broad spectral bands (Yang 2002).

To resolve the confusions in spectral signals, hierarchical classification and spatial reclassification procedures were developed with full consideration of the imaging sensor and the scenic characteristics. This section describes the procedures used for hierarchical classification, and the next section focuses on spatial reclassification. Hierarchical classification emphasizes the use of image subsets that are organized hierarchically, rather than whole scenes, in a series of independent classification procedures. The purpose of using image subsets is to isolate the problem (i.e. spectral confusion) categories from others so that the most effective classification decision can be developed for each subset. Apparently, hierarchical classification allows each form of information to be used in its most effective context (Campbell 2002). The hierarchical classification developed here consists of a number of procedures, as discussed in the following sections (figure 3).

2.5.1 ISODATA clustering. The ISODATA (Interactive Self-organizing Data Analysis) algorithm was used to identify spectral clusters from image data excluding the thermal band. To avoid the impacts of sampling characteristics, the ISODATA algorithm was implemented without assigning predefined signature sets as starting clusters. Each scene was grouped into 60 spectral clusters when the convergence value reached at least 0.990.

2.5.2 Landscape segmentation. Each cluster map, i.e. the output after ISODATA clustering, was separated into urban and rural regions through the use of an image 'mask'. The mask was actually a binary image where urban area was defined with the use of road intersection density slices and road buffers through a three-step procedure. First, road intersections were extracted from the ESRI 2002 road networks (ESRI 2003) and a road intersection density surface was generated by spreading out these points. Note that the road data for 1989 and 1996 were derived from the ESRI 2002 road networks which were adjusted with the reference of the satellite images acquired at the two different years (see table 1). Secondly, a threshold density value was determined interactively so that most of the urban area could be included. Note that the determination of the urban area involved the procedure of visual image interpretation as described by Campbell (2002). With the threshold value available, the density map was sliced into two parts. Lastly, the portion with road intersection density beyond the threshold was unionized with 100 m road buffers so that the boundary of urban area was defined. Any area outside this boundary was defined as the rural region.

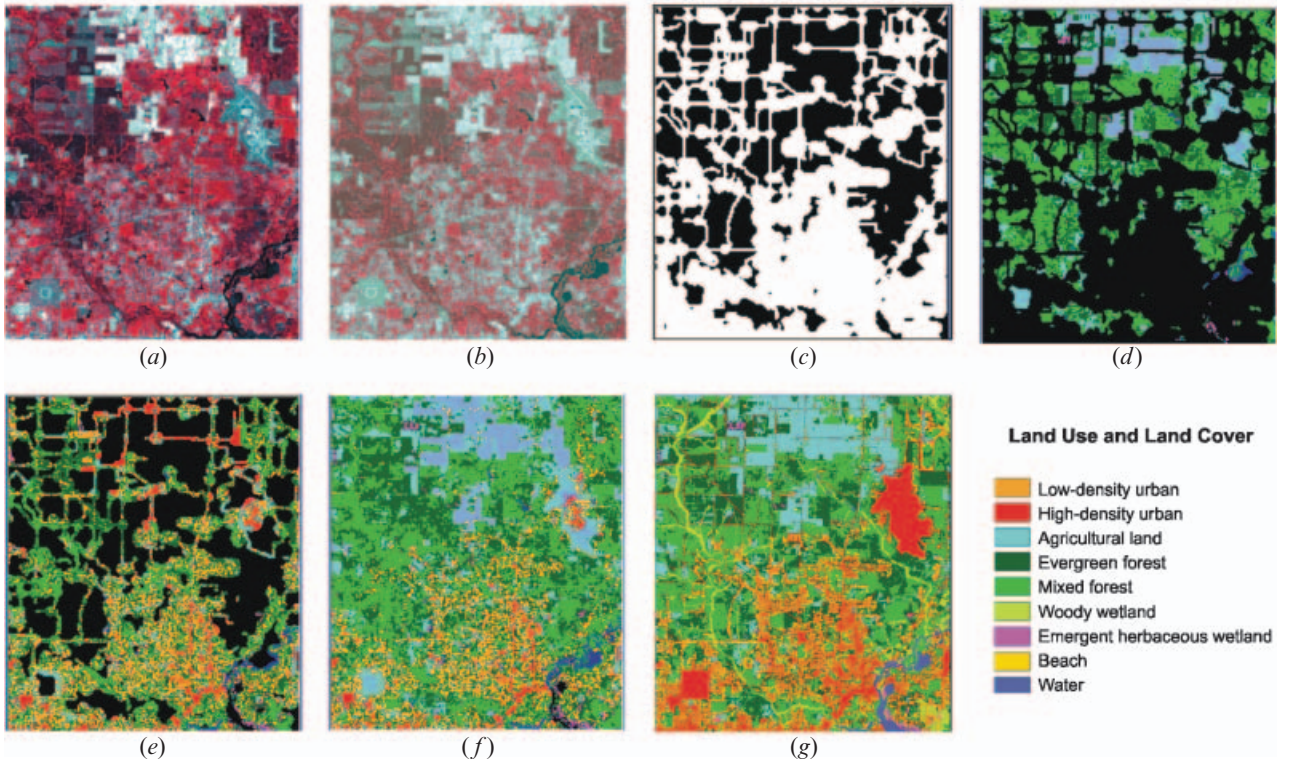

Figure 3. Sequential procedures used in land-use and land-cover classification. (*a*) The original image in false colour display. (*b*) The cluster image in false colour after ISODATA clustering. (*c*) The mask image consisting of road intersection density slices and road buffers. (*d*) The map for the rural part after cluster labelling. (*e*) The map for the urban part after cluster labelling. (*f*) The map after the merging of (*d*) and (*e*). (*g*) The final map after spatial reclassification through the use of image interpretation procedures, auxiliary data and a variety of GIS functions. Note that some pixels which were labelled wrongly were recoded into the right classes. Detailed discussion on these procedures can be found in the text.

2.5.3 Interactive classification. Each spectral cluster in either the urban or the rural portion was assigned into one of the nine land-use and land-cover classes using visual inspection of the original images, the reference data and the familiarity of the study area. To label the clusters, the original image in false colour composite (FCC) and the clustered map were displayed side by side and the displays were spatially linked. A targeted spectral class was highlighted in colour and its corresponding image pixels were examined by moving the cursor across the screen. The class assignment for individual clusters was based on an examination of the targeted cluster at two different levels of details. At the large-scale level, the individual image colour was mainly used in decision making. At the small-scale level, however, other image elements such as association and site were utilized to improve classification accuracy. The land-use and land-cover classifications of both the urban and rural portions were then combined to form a whole map. This was the initial land-use and land-cover classification.

2.6 *Spatial reclassification*

The initial land-use and land-cover maps after hierarchical classification came with the accuracies of approximately 70–75%. For this study, however, higher accuracy was needed. Therefore, further research effort was attempted to reduce image classification errors and improve accuracy. For this purpose, a spatial reclassification procedure has been developed to recode those pixels being labelled wrongly. Spatial reclassification was implemented through the use of image interpretation procedures, auxiliary data and a variety of GIS functions. It consists of several steps as described below.

2.6.1 Raster modal filtering. A 3×3 modal filter was used to reduce boundary errors at class boundaries due to the occurrences of intra-pixel spectral mixing and signal noises. Pixels identified as boundary errors are generally in the form of salt and pepper and they can be replaced with classes of their surroundings through a modal filter.

2.6.2 Iterative image interpretation. The level of spectral confusion described in Section 2.5 was substantially suppressed after hierarchical classification. However, a varying degree of spectral confusion was still observable in some areas. These areas were identified with an image interpretation procedure through which spectral and spatial contextual contents as well as human wisdom and experience were synthesized. Image interpretation can be incorporated effectively into a digital classification procedure with the use of on-screen digitizing, multiple zooming, AOI (area of interest) functionality and other relevant GIS tools such as overlaying and recoding. In addition, several image processing programs permit advanced tools for spatial modelling through which some 'manual' operations can be implemented automatically.

With the above methods, four major types of spectral confusion were identified:(i) low density urban (mostly residential)/mixed forest (sparse trees); (ii) low density urban (scattered residential)/agricultural land (sparse crops or grasses); (iii) mixed forest (sparse forest and shrubs)/agricultural land (cropland or grassland); and (iv) high density urban(large open roof buildings, air fields and multi-lane highways)/ barren land (large barren landmass, beaches, clearouts, and fallowed land). These pairs of land-use and land-cover types were spectrally similar to varying degrees. Whenever any spectrally confused cluster was identified, an AOI layer was

immediately created through on-screen digitizing to define a 'mask' by which the problematic cluster was split and then recoded into a correct land-use and land-cover class. This process was iterative until an acceptable accuracy was reached.

2.6.3 GIS data overlay enforcement. Several GIS data layers were overlaid with the image classification product after the above procedures were completed, which included: (i) weighted buffers of road networks for 1989, 1996 and 2002, respectively. Road data were derived from the ESRI 2002 road network adjusted with the reference of three image scenes (see table 1); (ii) airports, military fields, tourism and recreational facilities for the above three years. They were initially extracted from the 1995 FDEP land-use and land-cover map (see Section 2.2) and were then modified by using the three image scenes; and (iii) two types of wetlands which were extracted from NWI datasets for 1992 and then modified by using the above image scenes.

2.7 *Accuracy assessment*

The accuracy assessment was conducted through a standard method described by Congalton (1991). At least 50 test points per class were taken through a stratified random sampling scheme. The reference data used for accuracy assessment were described in Section 2.2. Producer accuracy, user accuracy and Kappa statistics were computed. Overall, all these maps met the minimum 85% accuracy stipulated by the Anderson classification scheme (Anderson *et al*. 1976). Detailed reports are shown in tables 2–4. This indicates that the image processing procedure developed here has been effective in producing compatible land-use and land-cover data through time. Final land-use and land-cover classification maps for three different years are shown in figure 4. The statistics for each classification map are shown in figure 5 and table 5, respectively.

2.8 *Change detection*

Procedures were developed to detect changes in landscape spatial pattern and to examine the nature of change. For spatial pattern analysis, the focus was on the development of low density urban use as well as the growth of mixed forest land (figure 6). Both classes show relatively larger magnitude of changes during the period 1989–2002 when compared with other categories. Figures 6(*a*) and (*b*) were produced with GIS minimum dominate overlay function by which the smallest amount of land use and land cover in 1989 shows up fully while only the net addition in the following years of the time sequence is displayed. For example, the green-coloured patches represent the net additions of low density urban use or mixed forest during the periods 1989 and 1996.

Analysing land-use and land-cover conversion allows different combinations of changes to be revealed, thus providing further information concerning the nature of change. A two-way cross-tabulation or matrix analysis was adopted to characterize land-use and land-cover conversions. This analysis produces a thematic layer that contains a separate class for every coincidence in two layers. There are many possible combinations but this study focuses on the conversions of forest, agricultural land, or wetlands into urban uses as well as the conversion of evergreen forest into mixed forest. Thus, only 11 combinations were scrutinized for further analysis. The remaining combinations were merged into a single unit (table 6). The map showing the above conversions can be seen in figure 7.

Table 2. The accuracy assessment report for the 1989 map.

Land use/cover	Low density urban	High density urban	Agricultural land	Evergreen forest	Mixed forest	Woody wetlands	Emergent herbaceous wetlands	Barren land	Water	Row total
Low density urban	**36**	5	5	2	1			1		50
High density urban	12	**229**	6		3					250
Agricultural land	2		**96**	2						100
Evergreen forest				**48**	2					50
Mixed forest				2	**48**					50
Woody wetlands					2	**47**			1	50
Emergent herbaceous wetlands		1	2			5	**41**		1	50
Barren land							1	**48**	1	50
Water									**100**	100
Column total	50	235	109	54	56	52	42	49	103	750
Overall Accuracy=92.40%						**Overall K Coefficient of Agreement=0.91**				
		Producer's accuracy (%)		User's accuracy (%)		Conditional K Coefficient of Agreement				
Low density urban		72.00		72.00		Low density urban			0.70	
High density urban		97.45		91.60		High density urban			0.88	
Agricultural land		88.07		96.00		Agricultural land			0.95	
Evergreen forest		88.89		96.00		Evergreen forest			0.96	
Mixed forest		85.71		96.00		Mixed forest			0.96	
Woody wetlands		90.38		94.00		Woody wetlands			0.94	
Emergent herbaceous wetlands		97.62		82.00		Emergent herbaceous wetlands			0.81	
Barren land		97.96		96.00		Barren land			0.96	
Water		97.09		100.00		Water			1.00	

Table 3. The accuracy assessment report for the 1996 map.

Land use/cover	Low density urban	High density urban	Agricultural land	Evergreen forest	Mixed forest	Woody wetlands	Emergent herbaceous wetlands	Barren land	Water	Row total
Low density urban	**40**	3	2	2	1	2				50
High density urban	12	**234**						4		250
Agricultural land	1		**98**	1						100
Evergreen forest			1	**49**						50
Mixed forest			1	1	**48**					50
Woody wetlands						**47**	1		2	50
Emergent herbaceous wetlands					2	1	**46**		1	50
Barren land								**50**		50
Water							3		**97**	100
Column total	53	237	102	53	51	50	50	54	100	750

Overall Accuracy=94.53% **Overall *K* Coefficient of Agreement=0.93**

	Producer's accuracy (%)	User's accuracy (%)	Conditional *K* Coefficient of Agreement
Low density urban	75.47	80.00	0.75
High density urban	98.73	93.60	0.91
Agricultural land	96.08	98.00	0.98
Evergreen forest	92.45	98.00	0.98
Mixed forest	94.12	96.00	0.96
Woody wetlands	94.00	94.00	0.94
Emergent herbaceous wetlands	92.00	92.00	0.91
Barren land	92.59	100.00	1.00
Water	97.00	97.00	0.97

Table 4. The accuracy assessment report for the 2002 map.

Land use/cover	Low density urban	High density urban	Agricultural land	Evergreen forest	Mixed forest	Woody wetlands	Emergent herbaceous wetlands	Barren land	Water	Row total
Low density urban	**39**	1	3	4	3					50
High density urban	5	**239**	3	2	1					250
Agricultural land	1		**96**	1	1			1		100
Evergreen forest	1		2	**45**	2					50
Mixed forest					**50**					50
Woody wetlands					1	**48**	1			50
Emergent herbaceous wetlands				1			**48**		1	50
Barren land		2	3					**45**		50
Water		1			1		2		**96**	100
Column total	46	243	107	53	59	48	51	46	97	750
Overall Accuracy=94.13%						**Overall *K* Coefficient of Agreement=0.93**				
		Producer's accuracy (%)		User's accuracy (%)		Conditional *K* Coefficient of Agreement				
Low density urban		84.78		78.00		Low density urban			0.77	
High density urban		98.35		95.60		High density urban			0.93	
Agricultural land		89.72		96.00		Agricultural land			0.95	
Evergreen forest		84.91		90.00		Evergreen forest			0.89	
Mixed forest		84.75		100.00		Mixed forest			1.00	
Woody wetlands		100.00		96.00		Woody wetlands			0.96	
Emergent herbaceous wetlands		94.12		96.00		Emergent herbaceous wetlands			0.96	
Barren land		97.83		90.00		Barren land			0.89	
Water		98.97		96.00		Water			0.95	

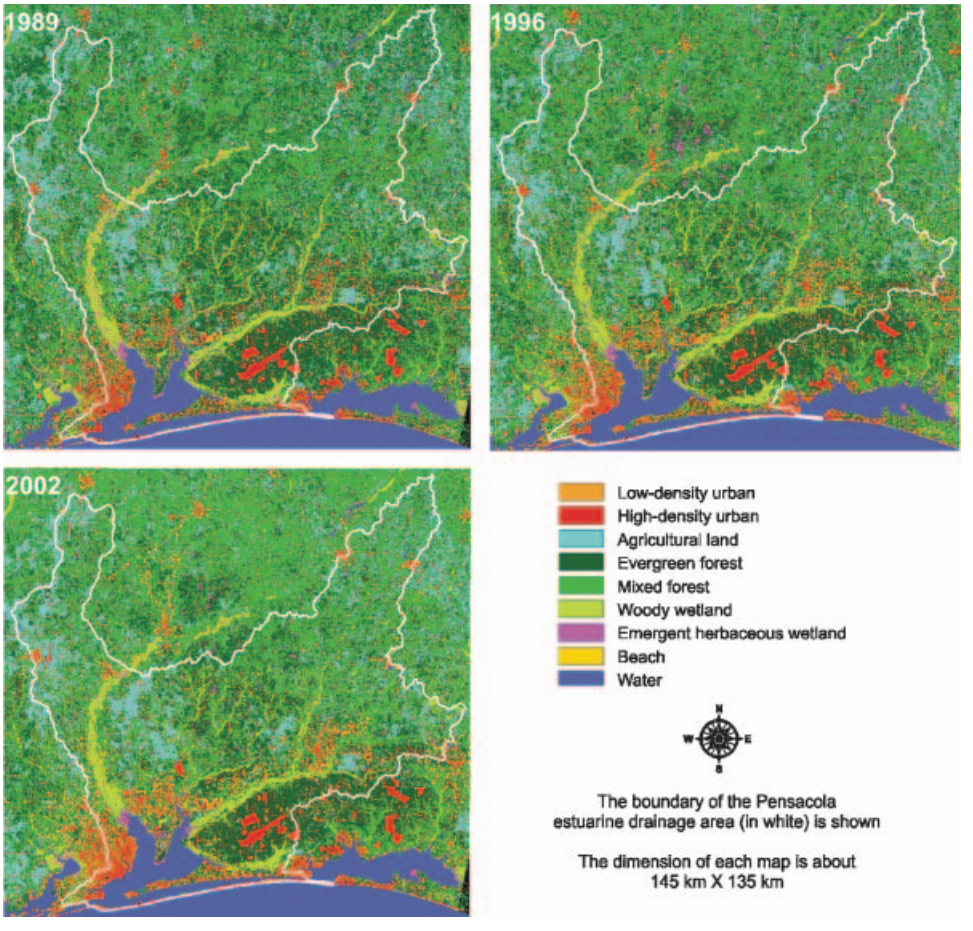

Figure 4. Land-use and land-cover maps for the Pensacola estuarine drainage area (PEDA): 1989–2002.

3. Results and discussion

Based on table 5 and figure 5, the classes of low density urban and mixed forest show the largest gains since 1989 for the Pensacola estuarine drainage area. In 1989, the low density urban use was small, occupying about 10 712 ha, or 1.17% of the total area (table 5). Although the low density urban showed the trend of spreading outward, its largest share was clearly located around the Pensacola bay and along the major highways such as I10 and US29 (figure 6(*a*)). Geographically, it was primarily concentrated within the counties of Escambia, Santa Rosa and Okaloosa. The spatial pattern of low density urban use in 1989 may be perceived as a form of concentration mixed with a certain degree of dispersal. Substantial growth of the low density urban land occurred in 1996 and 2002, with a net addition of 18 405 ha and 16 657 ha, respectively. Most of these new additions occurred in the Florida part (see figure 1). The spatial distribution pattern of low density urban use tended to be more dispersed. In quantitative terms, the low density urban land occupied 45 774 ha or 5.01% of the total area for the PEDA in 2002, indicating a 32.73% increase between 1989 and 2002. The weekly increment of low density urban use was

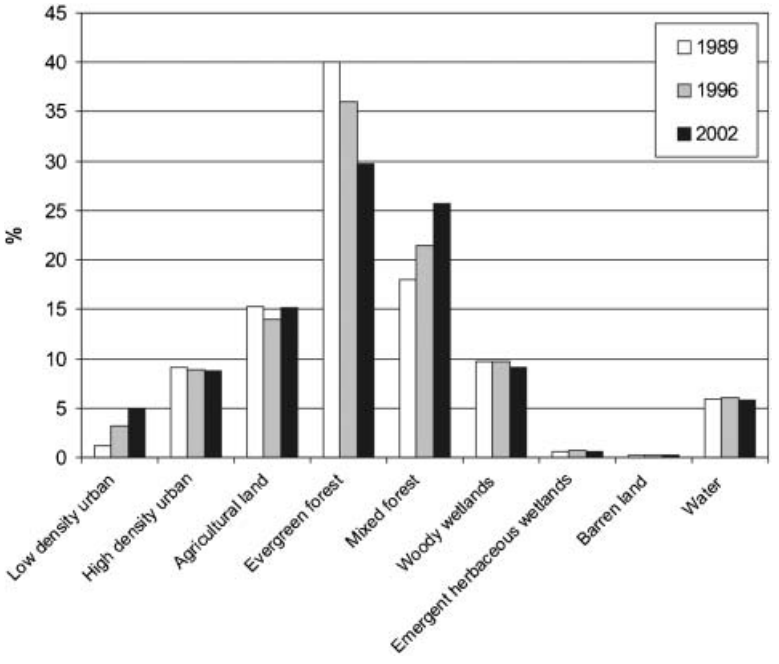

Figure 5. Land-use and land-cover changes for the Pensacola estuarine drainage area (PEDA) during the period 1989–2002.

approximately 52 ha or 129 acres for the same period. Undoubtedly, the fast development of low density urban use has been driven by the growth in population and housing units in the PEDA. During the last decade, the Pensacola metropolitan area alone had experienced 19.7% and 19.8% growth in population and housing units, respectively. Clearly, the rate of low density urban development surpassed that of population growth, indicating a major feature of the suburbanization process in the PEDA. On the other hand, the growth of low density urban use has been achieved at the cost of primary forest, agricultural land and wetlands (table 6). This has resulted in the replacement of vegetation with an enormous amount of impervious surface, which should definitely degrade water quality, biodiversity of aquatic systems, habitat structure and watershed health in the PEDA.

The mixed forest class has shown the largest gain among all the classes for the PEDA. In 1989, the mixed forest land occupied about 164 679 ha, or 18.02% of the total area for the PEDA (table 5). Significant increments occurred in 1996 and 2002, with a net addition of 31 010 ha and 38 932 ha, respectively. This represents a 42.47% increase between 1989 and 2002. Geographically, most of these new additions occurred in the upper part of the drainage area. A close examination of table 6 and figure 7 indicates that much of the gain was at the cost of evergreen forest, most likely through logging and harvesting operations. This suggests that forestry seems to be a very active land use in the upstream watershed. But it is unlikely that forest management would move land out of pine forest. Rather, early growth after cutting or clearing may result in more of a 'mixed' signature due to shrubs and brushes being present. By definition, the mixed forest class also contains a varying amount of shrubs, bushes and young trees. With the increase of the mosaic of various trees and shrubs, the forest landscape tends to be more fragmented. This should not only

Table 5. Land-use and land-cover statistics for 1989, 1996 and 2002, respectively.

	1989		1996		2002	
	ha	%	ha	%	ha	%
Low density urban use	10 712	1.17	29 117	3.19	45 774	5.01
High density urban use	82 838	9.07	80 669	8.83	79 663	8.72
Agriculture land	139 144	15.23	127 743	13.98	138 157	15.12
Evergreen forest	366 109	40.07	328 535	35.96	271 189	29.68
Mixed forest	164 679	18.02	195 689	21.42	234 621	25.68
Woody wetlands	88 692	9.71	88 940	9.73	83 289	9.12
Emergent herbaceous wetlands	5 889	0.64	6 058	0.66	5 938	0.65
Barren land	1 651	0.18	1 679	0.18	1 666	0.18
Water	53 992	5.91	55 281	6.05	53 401	5.84
Total	913 705	100.00	913 705	100.00	913 705	100.00

harm animals and plants, but also degrade water quality within the estuarine watershed.

Another significant change is the continuing decline in evergreen forest and woody wetlands in the Pensacola estuarine drainage area (table 5). The shrinking pattern of the spatial distribution of evergreen forest was proportional to the growth of low density urban use and mixed forest land described above (figure 7). In quantitative terms, evergreen forest occupied 366 109 ha or 40.07% of the total study area in 1989, which declined to 271 189 ha or 29.68% of the total area by 2002. This represents a decrease of 25.93%. Similarly, woody wetlands have declined from 88 692 ha (or 9.71%) to 83 289 ha (or 9.12%), thus representing a decrease of 6.1%, or a weekly rate of 8 ha (or 20 acres) in land area. The decline of evergreen forest and woody wetlands was clearly the result of the intensification of human activities in combination with continued urban development of the Pensacola metropolitan area through the process of suburbanization. On the other hand, the loss of wetlands should shrink the buffer zone that intercepts and filters polluted run-off before it can degrade the coastal water quality in the PEDA.

4. Conclusions

The impacts of intensifying human economic activities and the concentration of human population into estuarine areas are being felt throughout the world in both developing and developed countries alike. Information about changing patterns of land use and land cover through time in estuarine drainage areas is therefore important, not only for the management and planning of these areas, but also for a better understanding of the relationship between landscape dynamics and estuarine ecosystem responses. Satellite remote sensing allows a retrospective, synoptic viewing of large regions, thus providing the potential for a geographically and temporally detailed assessment of land-use and land-cover changes in estuarine watersheds.

By using the Pensacola estuarine drainage area as a case, this study has demonstrated the usefulness of satellite remote sensing, digital image processing and GIS techniques for coastal land-use and land-cover change mapping. The methodology developed here to map land use and land cover from a time series

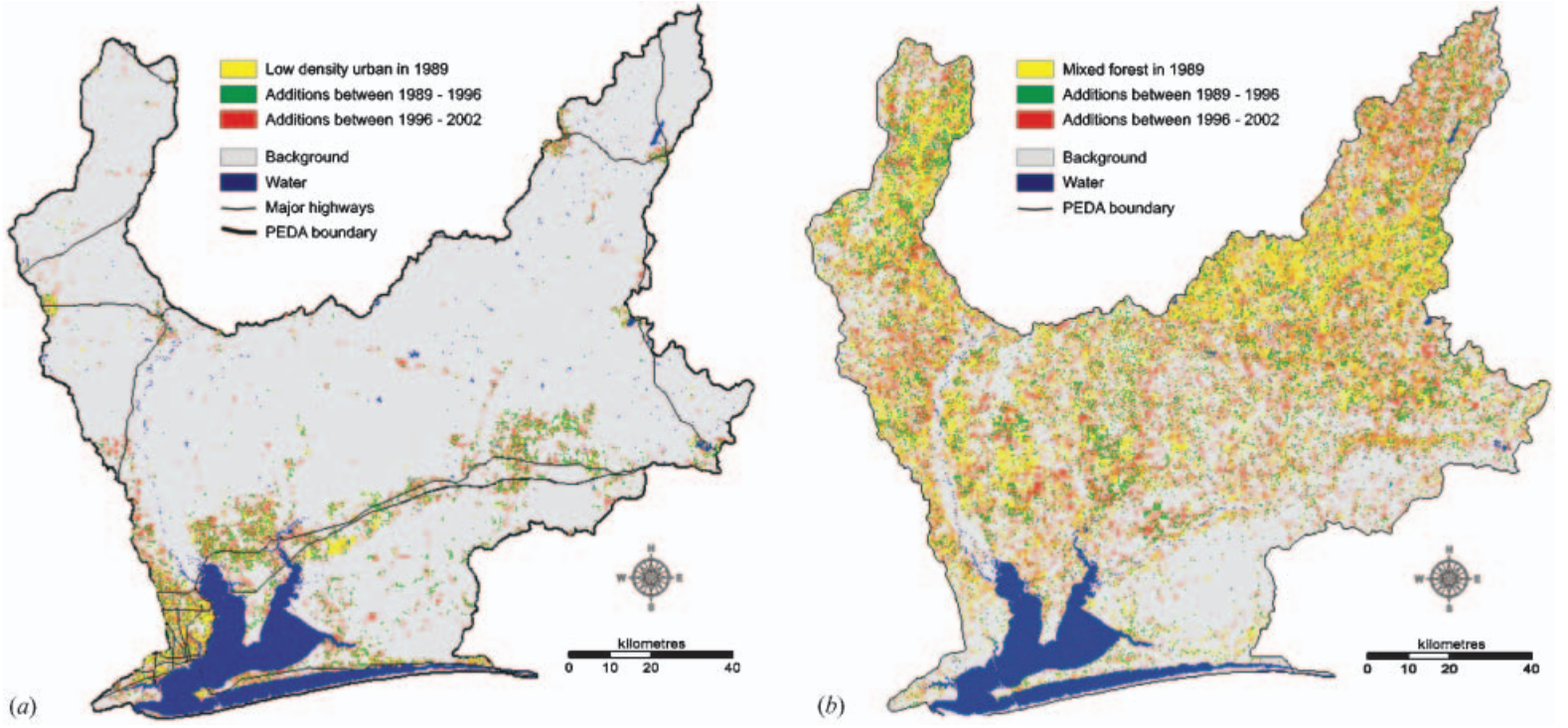

Figure 6(*a*). Spatial growth of low density urban use for the Pensacola estuarine drainage area (PEDA) during 1989 and 2002. Note that the major highways are also shown, along with the PEDA's boundary. (*b*). Spatial growth of mixed forest land for PEDA for the same period. The PEDA's boundary is also shown.

Table 6. Land-use and land-cover conversion statistics for the Pensacola estuarine drainage area during the period 1989–2002.

	Nature of change		Land conversation statistics	
Code	From	To	ha	%
C1	Agricultural land	Low density urban	4 587	0.50
C2	Evergreen forest	Low density urban	14 837	1.62
C3	Mixed forest	Low density urban	3 206	0.35
C4	Woody wetland	Low density urban	992	011
C5	Emergent herbaceous wetlands	Low density urban	192	0.02
C6	Agricultural land	High density urban	3 155	0.35
C7	Evergreen forest	High density urban	9 835	1.08
C8	Mixed forest	High density urban	3 701	0.41
C9	Woody wetland	High density urban	617	0.07
C10	Emergent herbaceous wetlands	High density urban	77	0.01
C11	Evergreen forest	Mixed forest	115 190	12.60
C0	All other combinations		757 301	82.88

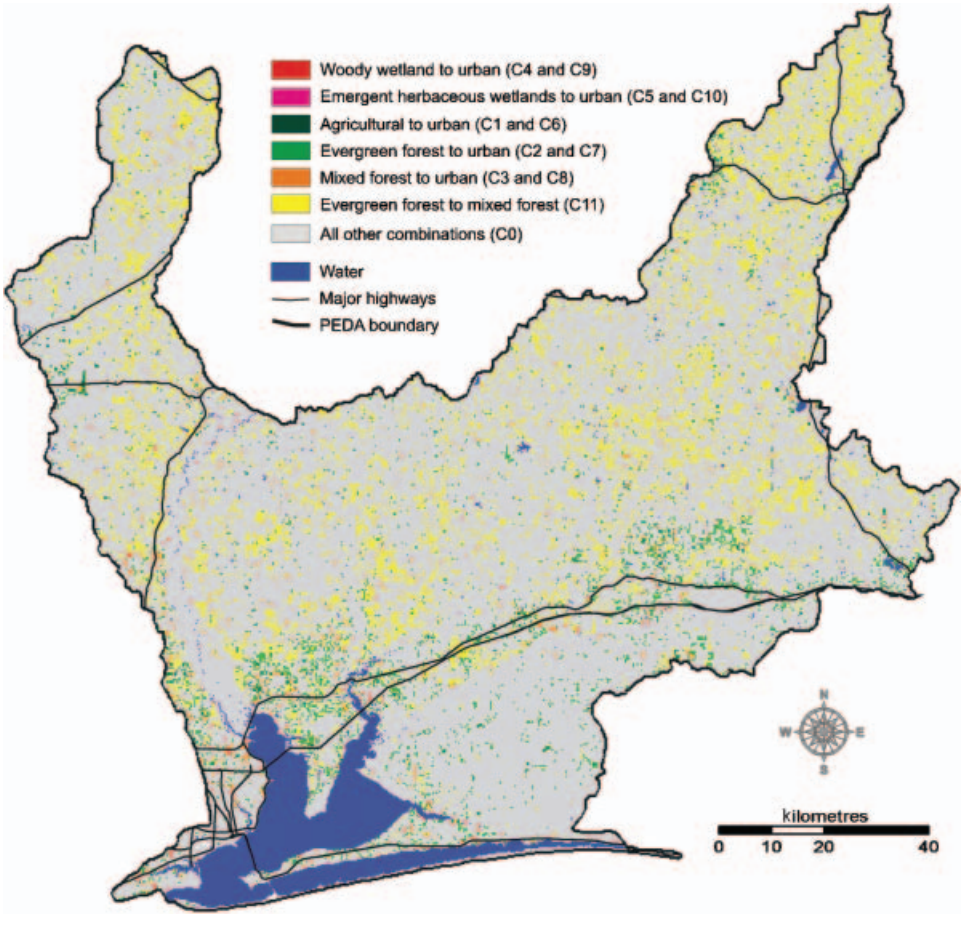

Figure 7. Land-use and land-cover conversions for the Pensacola estuarine drainage area (PEDA) during the period 1989–2002. Some conversion classes shown in table 6 are combined to simplify the visual complicity. Note that major highways are also shown.

of satellite images was based on an adequate understanding of landscape features, sensor characteristics and information extraction techniques. Several techniques have been adopted to ensure accurate image classification from the multi-temporal satellite data. The TM/ETM+ data were radiometrically normalized in order to establish a common radiometric response among the time series. To minimize the problem of spectral confusion, hierarchical classification and spatial reclassification techniques were developed. In hierarchical classification, an image 'mask' consisting of road intersection density slices and road buffers was used to separate each cluster (i.e. output after ISODATA clustering) into urban and rural portions. The class labelling was conducted for each portion independently and, later, both were merged to form a whole map. This procedure should help suppress the confusion in spectral signals between some urban and rural classes. In spatial reclassification, image interpretation procedures, auxiliary data and a variety of GIS functions were used to recode those pixels being labelled wrongly. Accuracy assessment confirmed that the image processing procedures were effective in extracting land-use and land-cover maps and statistics of the PEDA from the time series of Landsat TM/ETM+ data. Additionally, the combined use of post-classification comparison and GIS techniques has made possible the production of single-theme change maps, which emphasize spatial dynamics.

This study has also established a well-documented regional case study focusing on the Pensacola estuarine drainage area, one of few exemplary large-scale river-driven estuarine systems across the northern Gulf of Mexico. The project has revealed that a substantial increase in urban land occurred in the lower drainage basin in connection with population and housing growth. The increase in mixed forest land in the upstream watershed indicates that the forest landscape became more fragmented as a result of logging and harvesting operations. The shrinking pattern of the spatial distribution of evergreen forest was found to be proportional to the growth in low density urban use and mixed forest. Undoubtedly, the decline of evergreen forest and woody wetlands was clearly the result of the intensification of human economic activities in combination with fast urban development of the Pensacola metropolis through the process of suburbanization. These losses should compromise safeguards for water quality, biodiversity of aquatic systems, habitat structure and watershed health in the Pensacola estuarine drainage area. These findings should be useful not only to those who study estuarine dynamics but also to those who must manage and provide services in this highly sensitive ecosystem. Given that many estuaries face the growing problems caused by excess nutrients flowing from upstream watersheds, the land-use and land-cover mapping framework developed in the current study focusing on Pensacola bay can be applicable easily to other estuarine drainage basins. This can improve understanding of the variation in the nature–society dynamics of landscape, thus facilitating a sophisticated approach to estuarine environmental management and sustainable development.

Acknowledgements

This research has been supported by a grant from the US Environmental Protection Agency's Science to Achieve Results (STAR) Estuarine and Great Lakes (EaGLe) program through funding to the CEER-GOM, US EPA Agreement R829458. Although the research described in this article has been funded wholly or in part by the United States Environmental Protection Agency, it has not been subjected to the Agency's required peer and policy review and therefore does not necessarily reflect

the views of the Agency and no official endorsement should be inferred. The authors wish to thank several anonymous reviewers for their comments that helped improve the quality of the manuscript.

References

ANDERSON, J.R., HARDY, E.E., ROACH, J.T. and WITMER, R.E., 1976, *A Land Use and Land Cover Classification System for Use with Remote Sensor Data* (Sioux Falls, SD, USA: USGS Professional Paper 964).

BARNSLEY, M.J. and BARR, S.L., 1996, Inferring urban land use from satellite sensor images using kernel based spatial reclassification. *Photogrammetric Engineering and Remote Sensing*, **62**, pp. 949–958.

BASNYAT, P., TEETER, L.D., FLYNN, K.M. and LOCKABY, B.G., 1999, Relationships between landscape characteristics and nonpoint source pollution inputs to coastal estuaries. *Environmental Management*, **23**, pp. 539–549.

BOESCH, D.F., 2001, Agriculture and Coastal Eutrophication. Available online at: http://ian.umces.edu/commonground/coastaleu.pdf (accessed 20 December 2004).

BOWEN, J.L. and VALIELA, I., 2001, The ecological effects of urbanization of coastal watersheds: historical increases in nitrogen loads and eutrophication of Waquoit Bay estuaries. *Canadian Journal of Fisheries and Aquatic Sciences*, **58**, pp. 1489–1500.

CAMPBELL, J.B., 2002, *Introduction to Remote Sensing*, 3rd edn (New York: Guiford Press).

CHEN, X.W., 2002, Using remote sensing and GIS to analyze land cover change and its impacts on regional sustainable development. *International Journal of Remote Sensing*, **23**, pp. 107–124.

CONGALTON, R., 1991, A review of assessing the accuracy of classification of remotely sensed data. *Remote Sensing of Environment*, **37**, pp. 35–46.

DOJIRIA, M., YAMAGUCHI, M., WEISBERG, S.B. and LEE, H.J., 2003, Changing anthropogenic influence on the Santa Monica Bay watershed. *Marine Environmental Research*, **56**, pp. 1–14.

EPA, 1999, *The Ecological condition of Estuaries in the Gulf of Mexico* (EPA Publication 620–R-98-004).

ESRI, 2003, *ESRI Data & Maps 2002. Available online at: http://www.esri.com/data/datacd02.html (accessed 20 December 2004).*

FINKL, C.W. and CHARLIER, R.H., 2003, Sustainability of subtropical coastal zones in southeastern Florida: Challenges for urbanized coastal environments threatened by development, pollution, water supply, and storm hazards. *Journal of Coastal Research*, **19**, pp. 934–943.

FLORIDA DEPARTMENT OF ENVIRONMENTAL PROTECTION (FDEP), 2004, *NWFWMD 1995 Land Use.* Available online at: ftp://ftp.dep.state.fl.us/pub/gis/data/nwfwmd_landuse_1995.zip (accessed 20 December 2004).

GONZALEZ, O.M.R., 2001, Assessing vegetation and land cover changes in northeastern Puerto Rico: 1978–1995. *Caribbean Journal of Science*, **37**, pp. 95–106.

HALL, F.G., STREBEL, D.E., NICKESON, J.E. and GOETZ, S.J., 1991, Radiometric rectification: toward a common radiometric response among multidate, multisensor images. *Remote Sensing of Environment*, **35**, pp. 11–27.

HEROLD, M., LIU, X. and CLARKE, K.C., 2003, Spatial metrics and image texture for mapping urban land use. *Photogrammetrical Engineering and Remote Sensing*, **69**, pp. 991–1002.

JENSEN, J.R., 2004, *Introductory Digital Image Processing: A Remote Sensing Perspective* (New Jersey: Pearson Prentice Hall).

LAKSHMI, A. and RAJAGOPOLAN, R., 2000, Socio-economic implications of coastal zone degradation and their mitigation: a case study from coastal villages in India. *Ocean & Coastal Management*, **43**, pp. 749–762.

MARSH, O.T., 1966, *Geology of Escambia and Santa Rosa Counties, Western Florida Panhandle (Florida Geological Survey Bulletin 46)*.

NFWMD, 1997, *The Pensacola Bay System Surface Water Improvement and Management Plan* (Program Development Series 97-2).

NIEMI, G., WARDROP, D., BROOKS, R., ANDERSON, S., BRADY, V., PAERL, H., RAKOCINSKI, C., BROUWER, M., LEVINSON, B. and MCDONALD, M., 2004, Rationale for a new generation of ecological indicators for coastal waters. *Environmental Health Perspectives*, **112**, pp. 979–986.

NOAA, 1999, *ORCA's Coastal Assessment Framework (CAF)*. Available online at: http://spo.nos.noaa.gov/projects/caf/caf.html (accessed 20 December 2004).

NRC, 2000, *Clean Coastal Waters: Understanding and Reducing the Effects of Nutrient Pollution* (Washington DC: National Academy Press).

O'HARA, C.G., KING, J.S., CARTWRIGHT, J.H. and KING, R.L., 2003, Multitemporal land use and land cover classification of urbanized areas within sensitive coastal environments. *IEEE Transactions on Geoscience and Remote Sensing*, **41**, pp. 2005–2014.

RAO, B.R.M., DWIVEDI, R.S., KUSHWAHA, S.P.S., BHATTACHARYA, S.N., ANAND, J.B. and DASGUPTA, S., 1999, Monitoring the spatial extent of coastal wetlands using ERS-1 SAR data. *International Journal of Remote Sensing*, **20**, pp. 2509–2517.

RUIZ-LUNA, A. and BERLANGA-ROBLES, C.A., 2003, Land use, land cover changes and coastal lagoon surface reduction associated with urban growth in northwest Mexico. *Landscape Ecology*, **18**, pp. 159–171.

SCHMIDT, K.S., SKIDMORE, A.K., KLOOSTERMAN, E.H., VAN OOSTEN, H., KUMAR, L. and JANSSEN, J.A.M., 2004, Mapping coastal vegetation using an expert system and hyperspectral imagery. *Photogrammetrical Engineering and Remote Sensing*, **70**, pp. 703–715.

SHI, H. and SINGH, A., 2003, Status and interconnections of selected environmental issues in the global coastal zones. *Ambio*, **32**, pp. 145–152.

SHI, Z., WANG, R.C., HUANG, M.X. and LANDGRAF, D., 2002, Detection of coastal saline land uses with multi-temporal Landsat images in Shangyu City, China. *Environmental Management*, **30**, pp. 142–150.

US FISH & WILDLIFE SERVICE (USFWS), 2004, National Wetland Inventory Wetlands Data. Available online at: http://www.nwi.fws.gov/downloads.htm (accessed 20 December 2004).

USGS, 1996, *Digital Orthophoto Standards. Available online at: http://rmmcweb.cr.usgs.gov/public/nmpstds/doqstds.html (accessed 30 November 2004)*.

USGS, 2004a, *Digital Raster Graphics. Available online at: http://topomaps.usgs.gov/drg/ (accessed 20 December 2004)*.

USGS, 2004b, *1:250,000-scale Hydrologic Units of the United States. Available online at: http://water.usgs.gov/GIS/metadata/usgswrd/XML/huc250k.xml (accessed 20 December 2004)*.

USGS, 2004c, *National Land Cover Characterization 2001 (NLCD 2001). Available online at: http://www.mrlc.gov/mrlc2k_nlcd.asp (accessed 20 December 2004)*.

YANG, X., 2002, Satellite monitoring of urban spatial growth in the Atlanta metropolitan area. *Photogrammetric Engineering and Remote Sensing*, **68**, pp. 725–734.

YANG, X. and LO, C.P., 2000, Relative radiometric normalization performance for change detection from multi-date satellite images. *Photogrammetric Engineering and Remote Sensing*, **66**, pp. 967–980.